

# Kinetic of Phenol Adsorption by Mesoporous MCM-41 Nanoparticles

Dhananjay Naidu, Pallabi Pattanaik, Anup Anang Das, Naresh Kumar Sahoo

**Abstract** - In the present study application of MCM-41 for removal of phenol was investigated. MCM-41 nano-adsorbent was synthesized and characterized by FTIR, XRD and SEM analysis. Adsorption isotherm experiment was performed in batch shake flask. The experimental data were analyzed using various isotherm models. Result reveals that, Langmuir isotherm model fitted the data very well for the removal of phenol by the MCM-41 adsorbents. The calculated dimensionless separation factor,  $R_L$  indicates that the adsorption of phenol onto MCM-41 was favorable. Pseudo-first order, pseudo-second order kinetic equations and intraparticle diffusion model were applied to analyze the adsorption kinetics of the MCM-41 at different initial phenol concentrations. It was found that the adsorption of phenol on to the MCM-41 follows the pseudo-second order kinetic. At an initial phenol concentration of 130 mg/l, more than 99% phenol, 93% COD along with 96% of toxicity removal were achieved. Thus, the synthesized mesoporous MCM-41 proved to be a potential candidate for removal of phenol from industrial wastewater.

**Keywords.** Adsorption; MCM-41; phenol; adsorption kinetics; intraparticle diffusion model; toxicity removal.

## I. INTRODUCTION

The rapid growth and development of industrial sectors is the major concern in the globe, which releases an enormous quantity of toxic phenolic pollutants to the receiving environment. In general phenolic wastewater are released from different industries such as; iron and steel plant, phenolic resin, pharmaceutical, petroleum refineries, wood preservative and pesticides [1-3]. Sometimes these pollutants leach from soil and surface water consequently contaminates groundwater [4]. The phenolic pollutants are known to be carcinogenic and teratogenic in nature. The permissible limit of these phenolic pollutants is fixed at 1  $\mu\text{g/l}$  [5]. Therefore, these pollutants ought to be removed before being released in to the environment.

Several techniques have been investigated for the removal of phenolic compounds from different synthetic and real industrial wastewater such as; bioremediation, advanced oxidation, electrochemical process and physico-chemical

**Revised Manuscript Received on September 14, 2019.**

**Dhananjay Naidu**, Department of Chemistry, Environmental Science and Technology Program, Institute of Technical Education and Research, Siksha'O'Anusandhan, (Deemed to be University), Bhubaneswar, Odisha, India.

**Pallabi Pattanaik**, Department of Chemistry, Environmental Science and Technology Program, Institute of Technical Education and Research, Siksha'O'Anusandhan, (Deemed to be University), Bhubaneswar, Odisha, India.

**Anup Anang Das**, Department of Chemistry, Environmental Science and Technology Program, Institute of Technical Education and Research, Siksha'O'Anusandhan, (Deemed to be University), Bhubaneswar, Odisha, India.

**Naresh Kumar Sahoo**, Correspondence Author, Department of Chemistry, Environmental Science and Technology Program, Institute of Technical Education and Research, Siksha'O'Anusandhan, (Deemed to be University), Bhubaneswar, Odisha, India. (Email: nareshsahoo@soa.ac.in)

separation. Among them, removal of pollutants using adsorption method is very promising and popular. Several adsorbents, for instance; activated carbon, clay and fly ashes have been extensively studied for phenol removal [6]. The mesoporous MCM-41 is a promising adsorbent which offers high surface area, numerous cylindrical pore structures with large pore volume [7,8]. Several toxic pollutants like chromium, lead and mercury etc are efficiently removed by mesoporous MCM-41 as adsorbent [9]. Though removal of different toxic compounds by adsorption methods is very popular however, phenolic compounds removal by MCM-41 not yet studied extensively so far.

In the present study, MCM-41 nanoparticle was synthesized, characterized and its kinetic of phenol adsorption was evaluated to increase the phenolic and efficiency of toxicity removal from contaminated wastewater. MCM-41 is a part of the mesoporous silicate family known as M41S. Metal silicate materials applied as molecular sieves have a wide range of (13–100Å) pores in hexagonal order. All such items are formulated by a liquid-tool crystal-templating system, which is then removed by calcination or acid dissolution from the organic template. The properties are characterized by organized ranges of preservative templates, and by changing the length of the surfactant's hydrocarbon chain, the pores are adjusted. Various surfactant/si relationships and molecular circumstances generate solids with standardized cylindrical pores in hexagonally ordered order (MCM-41), coating materials (MCM-50), three-dimensional pores as well as suggested Cuba Symmetry (MCM-48). Such components may be helpful for catalytic, electronic, optical, and magnetic purposes. Changes by functional molecules can lead to adsorbents of certain characteristics.

## II. EXPERIMENTAL

### 2.1 Materials

In the present investigation, analytical and laboratory grade of chemicals were employed. Particularly, cetyltrimethylammonium bromide (CTAB), Tetraethylortho silicate (TEOS), as well as other chemicals used were purchased from Sigma Aldrich, Hi-Media India and Merck India.

### 2.2 Analytical methods

Chemical oxygen demand (COD) of the collected samples was measured using closed reflux method [10] in a temperature controlled COD digester (HACH, USA). Measurement of phenol was performed by 4-aminoantipyrine method [10]. All other parameters were measured as described in APHA [10].

### 2.3 Toxicity Test

Percentage of toxicity removal was estimated by the Resazurin reduction method [11]. A mixed microbial consortium was employed to perform the toxicity test. The percentage toxicity of the before and after treatment of the synthetic wastewater was calculated as given below.

$$\% \text{Toxicity} = \left[ \frac{A - B}{C - B} \right] \times 100$$

Where, A denotes the absorbance of synthetic wastewater (OD at 610 nm); B represents the OD of the mixed microbial consortia without phenol and C stands for the OD of the reagent control.

$$E = 1 - \left[ \frac{\% \text{Toxicity}_i}{\% \text{Toxicity}_f} \right] \times 100$$

Where, E denotes % of toxicity removal, Toxicity<sub>i</sub> stands for the % of toxicity by the raw synthetic wastewater. Toxicity<sub>f</sub> represents the % of toxicity remaining after treatment with MCM-41.

### 2.4 Synthesis of MCM-41

The MCM-41 was synthesized as depicted [12]. In 120 ml of water 2.4 gram of cetyltrimethylammonium bromide (CTAB) was dissolved at room temperature with constantly stirring. Then 10.5 ml of NH<sub>3</sub> solution (25 %) was mixed under continuously stirring at 300 rpm followed by addition of 10.0 ml of tetra-ethyl-ortho silicate followed by stirring for 1 h. The milky slurry solution generated was filtered and washed repeatedly, and the obtained product was dried at 110° C for 24 h in a hot air oven. The oven dried product was calcinated at 550 °C for 5 h.

### 2.5 Characterization

The synthesized MCM-41 was characterized by FTIR spectra (Make: Japan, Model JASCO-4100). MCM-41 was analyzed by Powder X-ray diffraction (PXRD) technique (Rigaku Miniflex set at 30 kV and 15 mA) at a scanning rate of 2°/min in steps of 0.01° in 2θ range of 1-10° by using a Cu Kα radiation. Further, Transmission scanning electron micrograph (TEM) of the synthesized MCM-41 was performed by employing a LEO-1430VP electron microscope.

### 2.6 Effect of adsorbent dose

The effect of adsorbent dose was studied in a 250 ml Erlenmeyer flask by employing 50 mL of synthetic wastewater and at an optimum pH of 5.0. The adsorbent doses of each Erlenmeyer flask was varied in the range of 0.0125 - 0.125 gm. A control flask without any MCM-41 adsorbent was taken to estimate the loss due to volatilization. Under room temperature all the flasks were kept in a rotary shaker at 100 rpm. Sampling was collected at regular interval of time. The contents of the conical flasks

were centrifuged at 8000 rpm for 20 minutes followed by filtered through millipore 0.45 micron filter and the filtrates were analyzed for residual phenol concentration.

### 2.7 Effect of initial phenolic concentration

Batch mode experiments were carried out in a 250 ml Erlenmeyer flask with optimum amount of adsorbent dose of 2 g/L and varying initial phenolic concentration in the range of 150 - 300 mg/L. The pH of each flask was maintained at 5 and was kept in a rotary shaker at 100 rpm in room temperature. Samples were collected at regular interval of time and centrifuged at 8000 rpm for 20 min followed by filtration by millipore 0.45 μm membrane filter and used for analysis of residual phenol.

### 2.8 Adsorption isotherms

Adsorption isotherm experiments were carried out in batch shake flask with a adsorbent dose of 2.8 g/L at pH 5 and agitation speed of 98 rpm with varying initial phenol concentration [13]. At regular intervals of time samples were collected and analyzed for residual phenol concentration. The phenol removal data were fitted to different literature existing isotherm such as; Langmuir, Freundlich and Temkin adsorption isotherms.

### 2.9 Adsorption Kinetics

**2.9 a Lagergren's Pseudo First Order Kinetics:** In order to predict the mechanism involved in the adsorption process, investigation of batch adsorption kinetics is necessary. Lagergren's pseudo first order kinetic model has been usually employed for prediction of pollutant adsorption as given in the equation below [14].

$$\frac{dq}{dt} = k_1 (q_e - q) \quad (3)$$

Where, q denotes amount of pollutant adsorbed (mg/g) at any time t, q<sub>e</sub> denotes the equilibrium adsorption capacity of MCM-41 (mg/g) and k<sub>1</sub> stands for pseudo first order rate constant (h<sup>-1</sup>). The above equation is simplified as follow:

$$\ln \left( \frac{q_e}{q_e - q} \right) = k_1 t \quad (4)$$

Thus, from above equation the rate constant k<sub>1</sub> (h<sup>-1</sup>) can be estimated from the plot of ln(q<sub>e</sub>/q<sub>e</sub>-q) versus time.

**2.9 b Pseudo Second Order Kinetics:** The pseudo second order kinetics proposed by Ho [15] is shown as follows.

$$\frac{dq}{dt} = k_2 (q_e - q)^2 \quad (5)$$

k<sub>2</sub> denotes Pseudo second order rate constant (g<sup>2</sup>mg<sup>-1</sup>min<sup>-1</sup>), the above Equation (5) can be simplified as follows;

$$\frac{t}{q} = \frac{1}{k_2 q_e^2} + \frac{1}{q_e} t \quad (6)$$

The value of the constants  $q_e$  (mg/g) and  $k_2$  (gmg<sup>-1</sup> h<sup>-1</sup>) can be estimated from plot between  $t/q$  versus  $t$ . Further, the initial adsorption rate  $h$  at  $t_0$  can be estimated as below:

$$h = k_2 q_e^2$$

**2.9 c Intraparticle Diffusion Model:** The intraparticle diffusion plot has been popularly used to study the mechanism involved during the process of pollutant adsorption. In literature, it was observed that the plot of  $qt$  versus  $t^{0.5}$  signify multi-linearity, which indicates multiple steps are associated during the process [16]. The intra-particle diffusion coefficient  $K_i$  can be expressed as follows:

$$K_i = \frac{q_t}{t^{0.5}} + C \quad (8)$$

Where,  $q_t$  denotes the quantity of phenol adsorption (mg/g) at time  $t$ .  $K_i$  stands for intraparticle diffusion rate constant.  $C$  denotes for the thickness of boundary layer. The intra-particle diffusion process is effective when the correlation coefficient obtained by fitting the experimental data to the equation 8 is close to one. The existence linear correlation between  $\log$  (% removal) and  $\log$  (time) further confirms the occurrence of intraparticle diffusion process [17]. In solid-liquid adsorption process, the transfer of solute was typically characterized by either external mass transfer or intraparticle diffusion or both.

### III. RESULTS AND DISCUSSION

#### 3.1 Characterization MCM-41 nanoparticles

Characterization of synthesized MCM-41 was carried out by FTIR, XRD and SEM analysis. FTIR spectra of the MCM-41 is shown (figure 1). The bending vibration of HOH caused by deformation vibrations of water molecules is appeared at 1634 cm<sup>-1</sup> [18]. The absorption band at 3460 cm<sup>-1</sup> indicates the stretching mode of water [19,20]. Similarly, the asymmetric extension vibration of siloxane groups (-Si-O-Si-) is observed at strong band near 1100 cm<sup>-1</sup>. Further, occurrences of strong peaks at 3460 and 1634 cm<sup>-1</sup> clearly indicates surfactant has been completely removed from the calcined MCM-41. The band near 2800-4000 cm<sup>-1</sup> reveals the presence of hydroxyl groups in the synthesized the MCM-41.

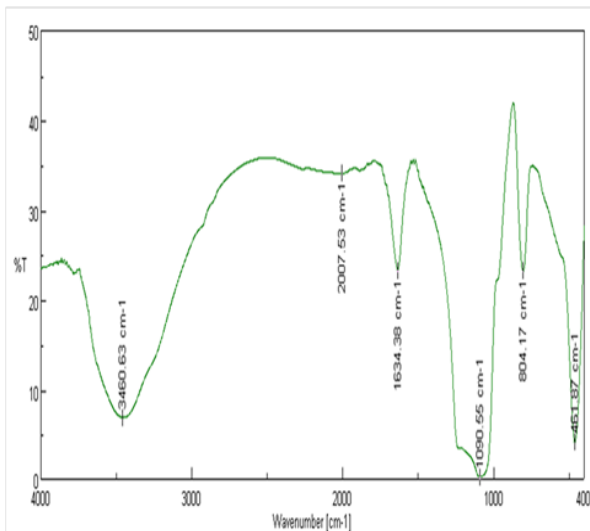


Figure 1. FTIR spectra of the synthesized MCM-41 nanoparticle.

The TEM image of the MCM-41 is given in (Figure 2) which reveals the well-ordered hexagonal array of mesoporous structure with pore size varies from 1.5 to 10 nm in diameter. The occurrence of uniformly distributed homogeneous mesoporous structure facilitates the uses of the MCM-41 as a better adsorbent.

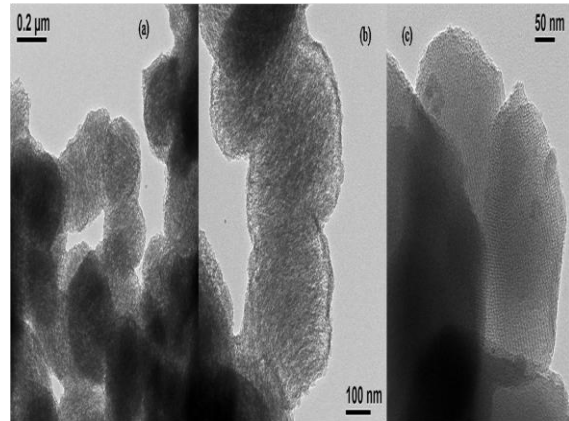


Figure 2. Transmission electron microscopic (TEM) images of the synthesized MCM-41 adsorbent.

The of the X-ray diffraction study of the synthesized MCM-41 nanoparticle and details about the crystal structure and phase composition has been discussed in our previous work [21]. The presence of hexagonal channel and mesoporosity nature of the synthesized MCM-41 was confirmed by the X-ray diffraction study.

#### 3.2. Adsorption Isotherms

##### 3.2 a Langmuir adsorption isotherm:

The Langmuir isotherm evaluates the amount of adsorbate adsorbed to form a unimolecular layer on the adsorbent surface. The linear forms of the Langmuir equation [22,23] is given as follows

$$1/q_e = 1/(q_0 b C_e) + 1/q_0$$

Where,  $q_0$  represents the maximum amount phenol adsorbed on to MCM-41 for formation a monolayer.  $C_e$  denotes concentration of phenol adsorbed at equilibrium condition. The constant term  $b$  stands for the binding energy constant and  $q_e$  is the amount phenol adsorbed per unit mass of MCM-41. The Langmuir adsorption isotherm is plotted between  $1/C_e$  versus  $1/q_e$  as demonstrated in the Figure 5. The values of  $b$  and  $q_0$  are determined from the slope and intercept of the straight line respectively. In the present investigation, the Langmuir constants is estimated as  $q_0 = 200$  mg/gm and  $b = -0.011$ .

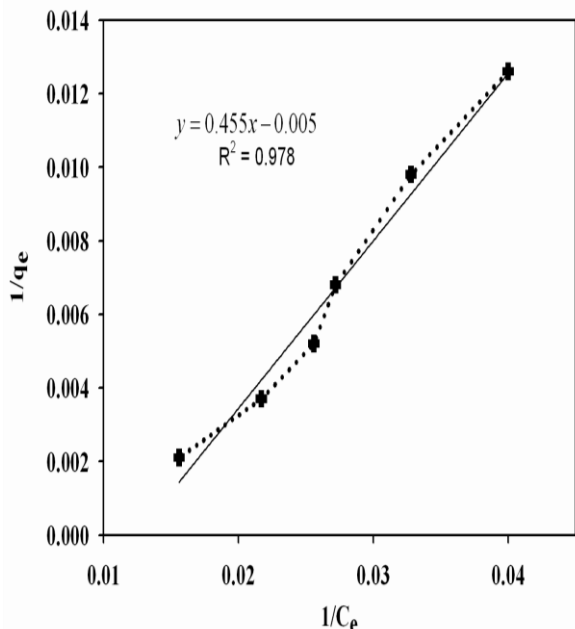


**Figure 5. Langmuir adsorption isotherm of synthetic wastewater for phenol removal by MCM-41.**

The dimensionless equilibrium parameter (r) is calculated by relating r with C<sub>0</sub> (initial phenol concentration) and Langmuir constant b as follows [24,25].

$$r = \frac{1}{(1 + bC_0)} \cdot 10$$

Table 1 represents the effect of dimensionless equilibrium parameter ‘r’ which reveals the extent of fit of the data obtained in present study to Langmuir isotherm.

**Table 1. The dimensionless equilibrium parameter ‘r’ and its relevance to Langmuir isotherm.**

‘r’ Value	Condition of isotherm	Initial phenol (C <sub>0</sub> ) (mg/L)	r = 1/(1+bC <sub>0</sub> )
r > 1	Unfavorable	100	10
r = 1	Linear	150	1.54
0 < r < 1	Favorable	200	0.83
r = 0	Irreversible	250	0.571
		300	0.434

The values of the ‘r’ indicate that, the adsorption process is unfavorable to fit with Langmuir isotherm at initial phenol concentration below 150 mg/l. On the other hand, when phenol concentration is more than 182 mg/l the indicates the experimental data’s is fitted Langmuir isotherm more precisely

**3.2b Freundlich adsorption isotherm:**

In Freundlich isotherm the adsorption process is regulates by the heterogeneous surface energy.

The linear transformation of Freundlich isotherm is given as follows:

$$\log q_e = \log K_f + \frac{1}{n} \log C_e \quad (11)$$

Where, q<sub>e</sub> represents the adsorption capacity (mg/g), C<sub>e</sub> (mg/l) stands for the equilibrium concentration of adsorbate. The constant terms ‘K<sub>f</sub> and n signify adsorption capacity and adsorption intensity of the adsorbent respectively.

The Freundlich isotherm is plotted between log C<sub>e</sub> against log q<sub>e</sub> as shown in Figure 6, which clearly designates that, the experimental data are fitted well to the Freundlich isotherm i.e. nearly a straight line with correlation coefficient of (R<sup>2</sup>) 0.985. The value of correlation coefficient clearly reveals that Langmuir isotherm fits the experimental data better than that of Freundlich isotherm. In the present study the values of 1/n i.e. 1.981 (≤ 1) indicates unfavorable nature of the Freundlich isotherm for phenol removal by synthesized adsorbent.

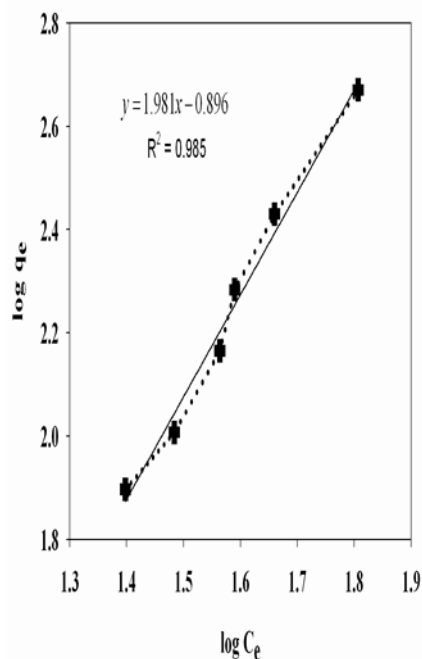


**Figure 6. Freundlich adsorption isotherms for phenol adsorption from synthetic wastewater by MCM-41.**

The value of K<sub>f</sub> (Freundlich constant) reveals affinity of the phenol adsorption on to MCM-41 as well as reflects the numbers of sportive sites [26]. In general, the Freundlich constant ‘n’ reveals the mutual interaction among the species adsorbed on to the adsorbent. For instance: the forces within the surface layers are attractive in nature when ‘n’ is more than unity, whereas it is ‘repulsive when ‘n’ is less than unity [27]. In the present investigation, the experimental value of ‘n’ is less than one (0.505) as calculated from the Freundlich isotherm, which clearly indicates the existence of repulsive forces between the adsorbed species. Therefore, it is clearly understood that

experimental data did not follow Freundlich adsorption isotherm. Since the values of  $1/n$  are calculated as 0.5 therefore it is well understood that intraparticle diffusion found to be the rate-limiting step in the phenol adsorption process by the MCM-41. It could be concluded that, the intraparticle diffusion is sufficiently high due to higher value of  $1/n$ , thus intraparticle diffusion is not the rate limiting step as revealed by the values of  $1/n$ . The  $1/n$  value reveals formation of weak bond between phenol and MCM-41 adsorbent as compared to polycinnamamide thorium (iv) phosphate viz. weak van der Waals force [28]. Further the estimated  $K_f$  value of 9.1 is relatively low than that of many literatures reported values further confirmed that, Freundlich isotherm did not fit well to the experimental data.

### 3.2 c Dubinin-Radushkevich isotherm:

In general, mechanism of adsorption cannot be interpreted by Freundlich and Langmuir adsorption isotherm constant. Therefore, in the present study Dubinin-Radushkevich (D-R) isotherm has been applied to understand the adsorption mechanism [29]. The non-linear form of D-R isotherm equation is shown in equation 12. The equation 12 was further simplified to linear form as shown in equation 13.

$$\ln q_e = \ln q_m - K \varepsilon^2 \quad 12$$

$$\varepsilon^2 = RT \ln \left( 1 + \frac{1}{C_e} \right) \quad 13$$

Where  $\varepsilon$  is Polanyi potential,  $q_e$  stands for the adsorption capacity,  $q_m$  is the theoretical adsorption capacity,  $K$  is Dubinin-Radushkevich constant related to adsorption energy,  $C_e$  is the concentration of phenol at equilibrium is the universal gas constant. (Figure 7) presented the plot of  $\ln q_e$  versus  $\varepsilon^2$  for removal of phenol by the MCM-41, which is found to be almost linear with regression coefficient ( $R^2$ ) of 0.987. The intercept and slope of the plot D-R isotherm plot represents the values of  $q_m$  and  $K$  constants respectively i.e. slope = zero (0) and intercept = 4.861 as illustrated in the (Figure 7). In the present study the  $K$  value is found to be zero (0) whereas,  $q_m$  is 496 mol/2kJ-2.

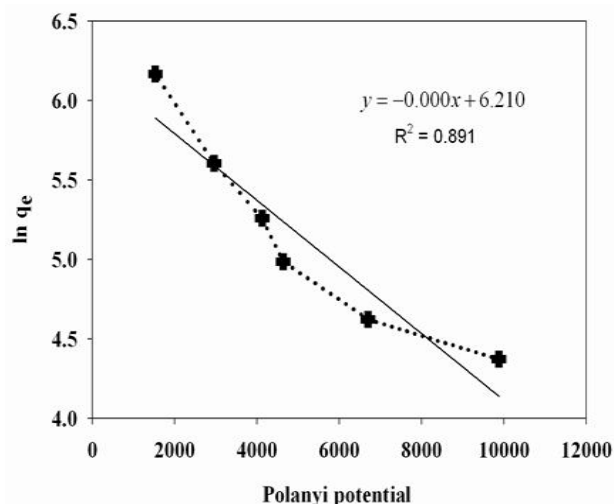


Figure 7. Dubinin-Radushkevich isotherm of synthetic wastewater for phenol removal by MCM-41.

### 3.2d Temkin adsorption isotherm:

In Temkin isotherm the adsorption energy declines linearly with surface coverage of the adsorbent, whereas, in Freundlich equation it varies in logarithmic form. The Temkin isotherm can be expressed as follows: [30].

$$q_e = \left( \frac{RT}{b} \right) \ln(A C_e) \quad 14$$

The linear transformation of Temkin equation is shown as follows:

$$q_e = B \ln A + B \ln C_e \quad 15$$

Where  $B = RT/b$  denotes the molecular interaction parameter,  $q_e$  is the adsorption capacity of the MCM-41 (mg/g) and  $C_e$  (mg/l) denotes unadsorbed phenol concentration at equilibrium conditions. The equilibrium constant is denoted by  $A$ .  $R$  denotes for the universal gas constant (8.314 J mol<sup>-1</sup>K<sup>-1</sup>) and  $T$  represents the absolute temperature. The Temkin constant  $b$  is associated with the heat of sorption [31].

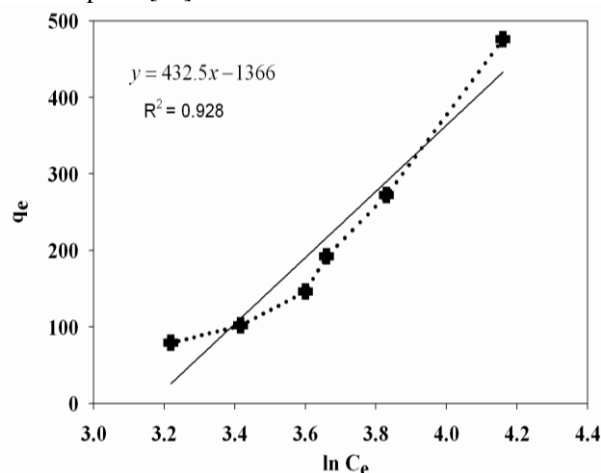


Figure 8. Temkin isotherm of synthetic wastewater for phenol removal by MCM-41.

Temkin isotherm associated with the molecular interactions among the adsorbed pollutant (phenol) and adsorbent surface (MCM-41) and the degree of heterogeneity of the adsorbent surface [32]. A plot of  $\ln C_e$  versus  $q_e$  is presented in the Figure 8 for phenol adsorption onto the synthesized MCM-41. The slope of the Temkin isotherm represents the molecular interaction parameter ( $B$ ) and is calculated to be 432.5 as shown in Figure 8. The values of Temkin isotherm constant  $A$  and  $b$  are estimated from the intercept and slope of the plot respectively. The values of  $A$  and  $b$  are estimated to be 23.38 and 5.86 respectively. The calculated interaction parameter  $B$  (432.5) is found to be significantly higher when compared with the 'B' values for polycinnamamide thorium (iv) polyacrylamide thorium (iv) phosphate (7.0) and phosphate (8.18) which strongly revealing stronger molecular interactions with the adsorbent and hence more phenol are adsorbed on the surface of the MCM-41. This may be due to presence of higher surface area of the mesoporous MCM-41 adsorbent. Further, calculated the 'b' value of MCM-41

is(5.86), considerably lower than that of many literature reported value i.e. 302,352, for polycinnamide thorium (iv) phosphate and polyacrylamide thorium (iv) phosphate. This clearly reveals that the heat of sorption during the adsorption of phenol by the MCM-41 is significantly low. The higher coefficient of determination (R<sup>2</sup>) of 0.928 reveals that the experimental data's are significantly satisfied the Temkin adsorption isotherm.

3.3 Adsorption Kinetics

The experimental data's are fitted very well to pseudo first order and pseudo second order kinetics models as shown in Figures 9 (a,b) and Figure 10 respectively. Table 2 represents the estimated values of the rate constants from the linear fitted pseudo first order and pseudo second order models together with the values of regression coefficients. From the Table 2 it is clearly examined that the linear correlation coefficients values are significantly high i.e. 0.965 and 0.937 which, reveals that the experimental data are very good fitted with pseudo first order model at both the phenol concentration tested in the study. However, pseudo second order model did not fit the experimental data with lower correlation coefficient value (R<sup>2</sup> = 0.239).

Table 2. The values of pseudo first order and pseudo second order rate constants for phenol adsorption on to MCM-41.

Adsorbent	T (K)	C <sub>0</sub> (mg/L)	k <sub>1</sub> (hr <sup>-1</sup> )	R <sub>1</sub> <sup>2</sup>	Q <sub>e</sub>	k <sub>2</sub> (g/mg hr)	h = k <sub>2</sub> q <sub>e</sub> <sup>2</sup>	R <sub>2</sub> <sup>2</sup>
MC M-41	30	15	0.1	0.9	50	4.4x10 <sup>-5</sup>	11	0.239
	5K	0	83	65	0			
	30	20	0.1	0.9	66	7.03x10 <sup>-3</sup>	32.247	0.965
	5K	0	71	37	67			

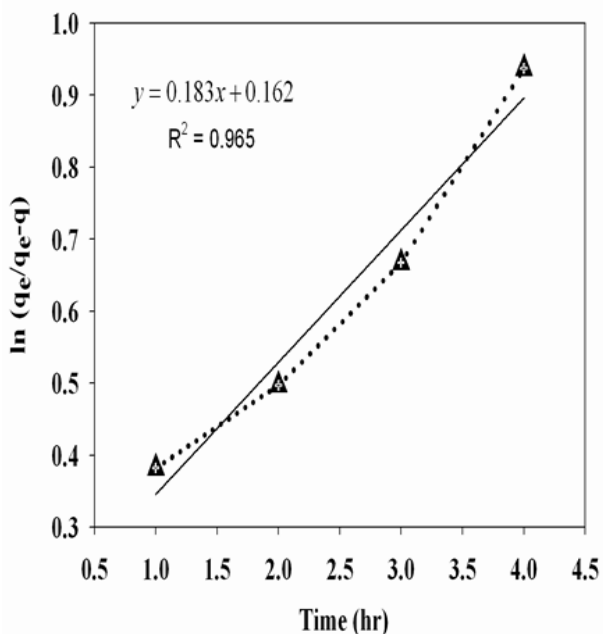


Figure 9 (a) Pseudo first order kinetic plots of phenol adsorption at 150 mg/L by MCM-41 at 305K.

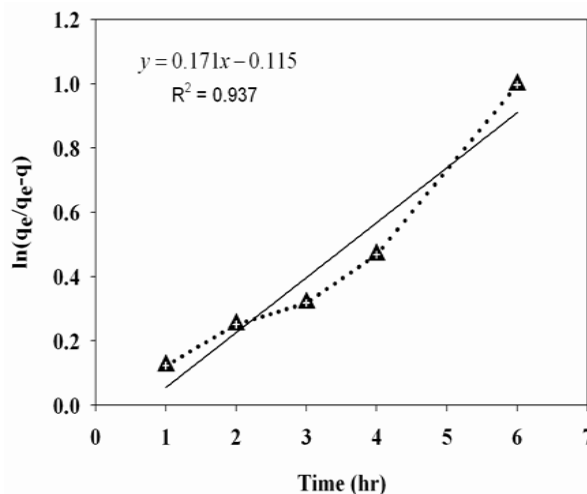


Figure 9(b). Pseudo first order kinetic plots of phenol adsorption at 200 mg/L by MCM-41 at 305K.

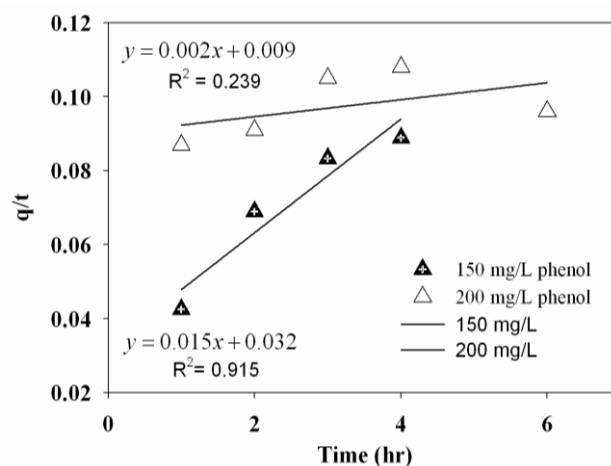


Figure 10. Pseudo second order kinetic plots of phenol adsorption at 150 mg/L and 200 mg/L by MCM-41 at 305K.

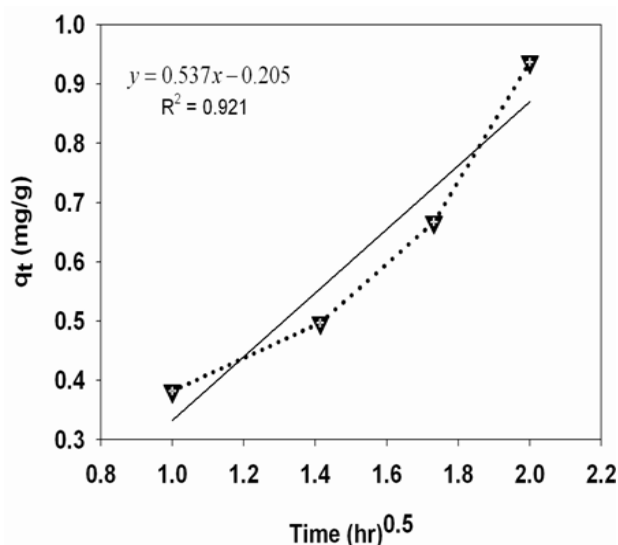
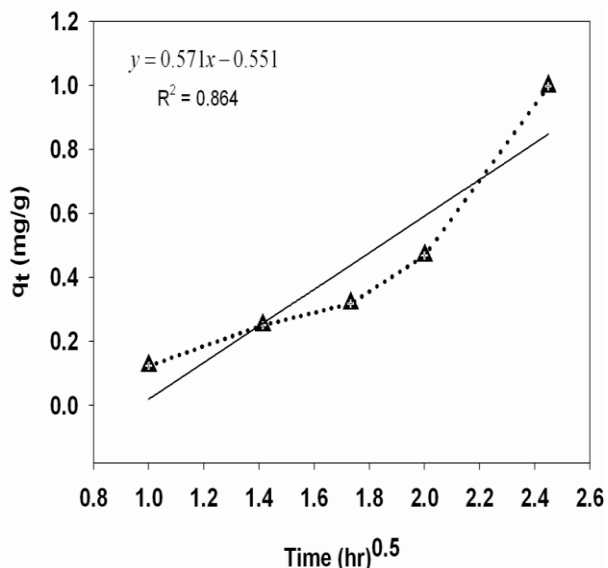


Figure 11 (a). Intraparticle kinetic plots of phenol adsorption at 150 mg/L by MCM-41 at 305K.



**Figure 11 (b). Intraparticle kinetic plots of phenol adsorption at 200 mg/L by MCM-41 at 305K.**

### 3.4 Intraparticle Diffusion

The intraparticle diffusion coefficients for phenol adsorption onto MCM-41 are deliberated

from the slope of the plot between square root of time (min<sup>0.5</sup>) versus amount of phenol adsorbed (mgg<sup>-1</sup>). In literature, many researchers reported that, the plot between qt versus t<sup>0.5</sup> correspond to multiple linearity, which signify the involvement of multiple steps during the pollutant adsorption process [14,16]. Figures 11 (a,b) demonstrated the plot between qt versus t<sup>0.5</sup> for adsorption of phenol at 150 mg/l and 200 mg/l respectively onto the MCM-41 nano-adsorbent. From these Figures, it is understood that, at all initial concentrations of phenol, the process of adsorption occurred in two phases i.e. an initial linear portion that completed with a smooth curve after that second linear portion. In the intraparticle diffusion plot the appearance of two phases reveals that the phenol adsorption on to MCM-41 progress by surface adsorption followed by intraparticle diffusion. The first curved portions of the plot signify the effect of boundary layer whereas, intra-particle or pore diffusion process of phenol adsorption on to MCM-41 is represents by the second linear portion of the curve. The intraparticle diffusion parameter  $K_i$  (mg/g hr<sup>0.5</sup>) can be estimated from the slope of the second linear portion of the curve whereas the effect of boundary layer can be evaluated by its intercept. Greater value of the intercept as shown in the Figures 11 (a,b), higher the surface adsorption process in the rate limiting step [33]. In the present study, intraparticle diffusion parameter  $K_i$  for phenol adsorption on to MCM-41 is calculated to be 0.744 and 0.970 mg-lh<sup>-10.5</sup> at 150mg/l and 200 mg/l of phenol respectively. Whereas, boundary layer parameter i.e. the intercept of the linear portion of the curve is estimated to be 0.576 and 1.406 at 150 mg/l and 200 mg/l of phenol respectively on to MCM-41. In general, the rate of adsorption governs by the slowest step i.e. either pore diffusion or film diffusion. In the earlier stages the adsorption of phenol onto MCM-41 might be regulated owing to film diffusion and when the phenol is loading on to the MCM-41 increases the adsorption process might be regulated because of intraparticle diffusion [33].

## IV. CONCLUSION

The FTIR spectrum of the synthesized MCM-41 has been confirmed the presence of functional groups such as hydrogen bonded OH groups, silanol groups (Si-OH). Similarly TEM micrographs reveals hexagonal mesoporous structure of the MCM-41, and which is further confirmed by the appearance of a strong diffraction peak at 2.30 (100 plane). The experimental data were very well fitted to the Langmuir and Temkin adsorption isotherms with a very high correlation coefficient value of greater than 0.9. The lower value of heat of sorption indicates the adsorption process is favorable. For enhancing its adsorption efficiency the sorption kinetics of phenol onto MCM-41 could be represented by the pseudo-second-order kinetic model. The phenol adsorption process is improved due the presence the mesoporous structure of MCM-41 which facilitates higher molecular interactions with the adsorbent. Further, the phenol adsorption on to MCM-41 is well described by a two-stage diffusion model. Therefore, the present investigation reveals that MCM-41 proved to be potential adsorbent for the removal of phenolic pollutants from industrial wastewaters.

## V. ACKNOWLEDGEMENTS

The authors acknowledge the financial support received from the Department of Biotechnology Government of India, New Delhi for execution of this research work.

## REFERENCES

- Sahoo N.K and Panigrahy N 2018 Environ Process. 2 287
- Tsai S.Y and Juang R.S 2006 J. Hazard. Mater. 138 125
- Bai J, Wen J.P, Li H.M and Jiang Y 2007 Proc. Biochem. 42 510
- Trapido M and Kallas J 2000 Environ. Technol. 21 799
- Sprenger C, Lorenzen G and Pekdeger A 2008 Occurrence and fate of microbial pathogens and organic trace compounds at riverbank filtration sites in Delhi, India., TECHNIAU.
- Khan N.A, Hasan Z and Jung S.H 2013 J. Hazard. Mater. 244444
- Chaliha S, Bhattacharyya K.G and Paul P 2008 Clean - Soil Air Water. 36488
- Zanjanchi M.A, Sajjadi H, Arvand M, Khah A.M and Choobar B.G 2011 Clean-Soil Air Water. 39 1007
- Cao J, Wu Y, Jin Y, Yilihan P and Huang W 2014 J-Taiwan-Inst-Chem-E. 45860
- APHA 2005 Standard Methods for the Examination of Water and Wastewater. 21 Washington DC
- Sahoo N.K, Pakshirajan K and Ghosh P.K 2011 J. Hazard. Mater. 190 729
- Parida K, Mishra K.G and Dash S.K 2012 J. Hazard. Mater. 241395
- Pattanaik P, Panigrahi N, Mishra J, Sahoo N.K, Dash B.P and Rath D 2018 J. Hazard. Toxic Radioact. 22 2
- Sivaraj R, Namasivayam C and Kadirvelu K 2001 Waste Manage. 21 105
- Ho Y.S 2003 Water Res. 37 2323
- Sun Q and Yang L 2003 Water Res. 37 1535
- Kannan K and Sundaram M. M 2001 Dyes Fig. 5125

## Kinetic Of Phenol Adsorption By Mesoporous Mcm-41 Nanoparticles

18. Pavia, D ,Lampman G.M and Kriz G.S 2001 Introduction to spectroscopy, Harcourt College Publisher,USA.
19. Hu Y, He Y, Wang X and We C 2014 Appl. Surf. Sci. 311825
20. Parvulescu V and Su B.L 2001 Catal. Today. 69 315
21. Naidu D, Panigrahi N, Mishra J and Sahoo N.K 2018 Int. J. Nano and Biomat.7 124
22. Das N, Pattanaik P and DasR 2005 J. Colloid. Inter. Sci.292 1
23. Mesina PV and Schuiz PC 2006 J.Colloid.Interface Sci. 299 305
24. Moufliha M, Akila A and Sebtib S 2005 J. Haz. Mat. B 119 183
25. Singh K.K, Talat M and Hasan SH 2006 Bioresour. Technol. 97 2124
26. Rao P.S and Bhole AG 2001 J. Ind. Water work assoc.99 100
27. Jaya R, Vivekanandan S and Lakshmi S 2010a Ind.J. Che. 40 115
28. Kannan N and Vanangamudi A 1991 Ind.J. Environ. Protec. 18 683
29. Eren E and Afsin B 2008 Dyes Pig. 76 220
30. Wang XS and Qin Y 2005 Proc. Biochem. 40 677
31. Akkaya G and Ozer A ,2005. Proc. Biochem. 40 3559
32. El-Shafei AA, Moussa MNH and El-Far AA 2001 Materials Chem. Phy. 70 175
33. Vadivelan V and Kumar K.V 2005 J. Colloid Int Sci.286 90.